Radiation Physics and Chemistry 175 (2020) 108049

Contents lists available at ScienceDirect

Radiation Physics and Chemistry

journal homepage: www.elsevier.com/locate/radphyschem

Silver clusters shape determination from in-situ XANES data

Janis Timoshenko[a,*], Stefanie Roese[b], Heinz Hövel[b], Anatoly I. Frenkel[a,c]

[a] Department of Materials Science and Chemical Engineering, Stony Brook University, Stony Brook, NY 11794, USA
[b] Fakultät Physik/DELTA, Technische Universität Dortmund, 44227 Dortmund, Germany
[c] Division of Chemistry, Brookhaven National Laboratory, Upton, NY 11973, USA

ARTICLE INFO

Keywords:
Nanoparticles
Cluster assembly
Shape determination
XANES
Machine learning
Neural networks

ABSTRACT

Knowledge of nanoparticle size, shape and morphology and of their in-situ transformations is crucial for establishing structure-properties relationship in nanosized materials that find applications, e.g., in plasmonic devices and heterogenous catalysis. Here we demonstrate that this information can be extracted reliably from in-situ X-ray absorption near edge structure (XANES) data, by combining ab-initio XANES simulations and machine learning (artificial neural network (NN)) approaches. Here we use NN-XANES method to extract information about the size, shape and interatomic distances in silver clusters, and to monitor their changes during the temperature-controlled particle aggregation.

1. Introduction

In addition to composition, structure and size, the shape of metallic NPs can also affect their properties, such as their atomic dynamics and thermal properties (Roldan Cuenya et al., 2010, 2011), electronic state (Behafarid et al., 2012) and catalytic activity (Mostafa et al., 2010; Roldan Cuenya, 2012; Narayanan and El-Sayed, 2004; Grunwaldt et al., 2000), plasmonic and optical properties (Tao et al., 2008; Kelly et al., 2003). Ability to determine reliably NPs shape is thus a step towards establishing structure-properties relationship in these materials. Important in this regard are in-situ studies of NPs shape, since NPs structure, size and shape can change in their expected working conditions, e.g., due to NPs coalescence or Ostwald ripening (Porsgaard et al., 2012; Newton et al., 2007) or interactions with the support and adsorbates (Grunwaldt et al., 2000; Newton et al., 2007; Hansen et al., 2002). The set of tools that enable accurate in-situ determination of NPs shape is, however, limited. (Roldan Cuenya, 2012).

Among those few, X-ray absorption spectroscopy (XAS) stands out as a premier method that is sensitive to the details of atomic arrangements and that can be employed in a broad range of experimental conditions (Van Bokhoven and Lamberti, 2016). Sensitivity of XAS to NPs shape has been demonstrated before (Roldan Cuenya et al., 2010; Mostafa et al., 2010; Roldan Cuenya et al., 2010; Frenkel, 1999; Frenkel et al., 2011, 2001). In these works for distinguishing between NPs shapes one relies on the analysis of coordination numbers (CNs), obtained by fitting extended X-ray absorption fine structure (EXAFS) data: NPs with different sizes, shapes and structures have different sets of corresponding particle-averaged CNs (Frenkel et al., 2001; Glasner and Frenkel, 2007; Jentys, 1999). For unambiguous determination of NPs shape, CNs not only for the first but also for more distant coordination shells are required (Frenkel et al., 2001; Glasner and Frenkel, 2007; Jentys, 1999). It is challenging, however, to extract them from EXAFS fitting. Many parameters are required to describe the overlapping contributions of distant shells and multiple scattering effects. This results in correlations in fitting variables and makes the procedure unstable. Such analysis of NPs shape is thus mostly limited to low-temperature studies of specially prepared model NPs, where EXAFS data of very good quality can be acquired.

Recently we demonstrated that for metallic particles CNs for the first few coordination shells can also be extracted from X-ray absorption near edge structure (XANES) by employing artificial neural network (NN) method (Timoshenko et al., 2017, 2018; Roese et al., 2018). Due to better signal-to-noise ratio in this portion of absorption spectra, good quality XANES data can be obtained in a broader range of experimental conditions, for more diluted samples and with better time resolution. XANES-based analysis is thus better suited for in-situ probing of NPs morphology. Here we apply NN method for interpretation of XANES data, collected in-situ during temperature-controlled aggregation of silver clusters embedded in room temperature ionic liquid (RTIL). Preliminary results for this system for the first coordination shell were published before (Roese et al., 2018). Here we focus on the analysis of distant coordination shells, and, for the first time, we employ our method for determination of NPs shape from their in-situ XANES spectra.

* Corresponding author.
E-mail address: janis.timosenko@stonybrook.edu (J. Timoshenko).

https://doi.org/10.1016/j.radphyschem.2018.11.003
Received 28 August 2018; Received in revised form 16 October 2018; Accepted 2 November 2018
Available online 05 November 2018
0969-806X/

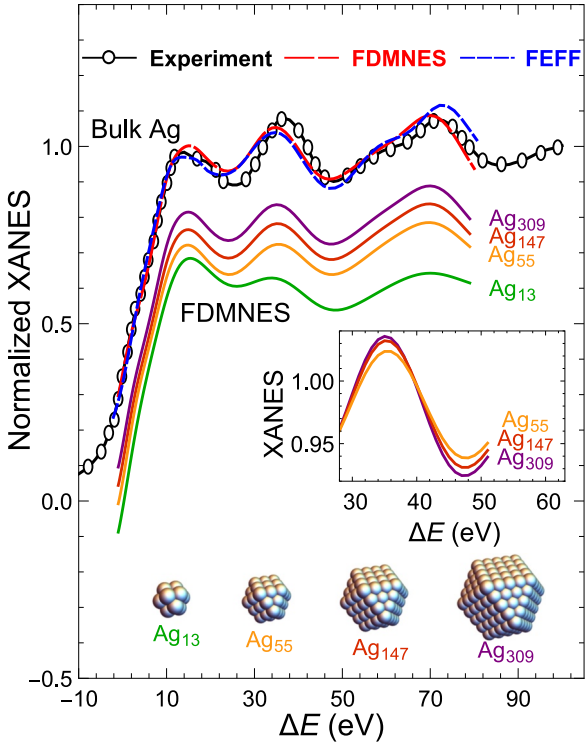

Fig. 1. Experimental Ag K-edge XANES for bulk silver and configuration-averaged spectra calculated with FEFF and FDMNES codes for bulk Ag and cuboctahedral Ag clusters with 13, 55, 147 and 309 atoms. Calculated spectra in the main panel are shifted vertically for clarity. The XANES region where the largest size effect is observed is zoomed in the inset.

2. Method description and validation

We follow the same procedure as in Ref. Timoshenko et al. (2017). NN is a composite function that can be trained to represent almost any relationship between NN input and output vectors by tuning the weights of different NN nodes (LeCun et al., 2015). In our case, the input vector is a discretized XANES spectrum. As the output we use CNs in the first three coordination shells ($\tilde{C}_1$, $\tilde{C}_2$, $\tilde{C}_3$), as well as the effective interatomic distance $\tilde{R}$. For NN training we use a set of XANES spectra, for which the true values of the structure parameters (C_1, C_2, C_3, R), are known. For this purpose we rely on ab-initio XANES modeling using FEFF (Rehr et al., 2010) and FDMNES (Bunău and Joly, 2009) codes. For Ag K-edge spectra in bulk Ag both codes provide good agreement with experimental data (Fig. 1).

For XANES simulations for Ag NPs with different sizes and shapes we use the same structure models with close-packed and icosahedral structures as in Refs. Timoshenko et al. (2017), Timoshenko et al. (2018). Theoretical simulations confirm the presence of particle size-effect in Ag K-edge XANES (Fig. 1), but it is relatively weak, especially for clusters larger than 1 nm. The non-linear sensitivity of NN to input features is thus crucial for reliable extraction of structural information.

To account for possible shortening of interatomic distances in small Ag NPs (Montano et al., 1984), atom coordinates in the structure models are rescaled to have nearest-neighbor distances in the range between 2.5 and 2.9 Å. In total, ca. 12,000 unique site-specific Ag K-edge XANES spectra were generated, which were further linearly combined, as explained in Refs. Timoshenko et al. (2017), Timoshenko et al. (2018), to increase the size of the training set to 200,000 spectra. See Refs. Timoshenko et al. (2017), Timoshenko et al. (2018) for technical details on NN implementation and training.

To validate the accuracy of the trained NN we apply it to another set of theoretical spectra for NPs of different sizes and shapes, which were not used for NN training. The good agreement between the known true

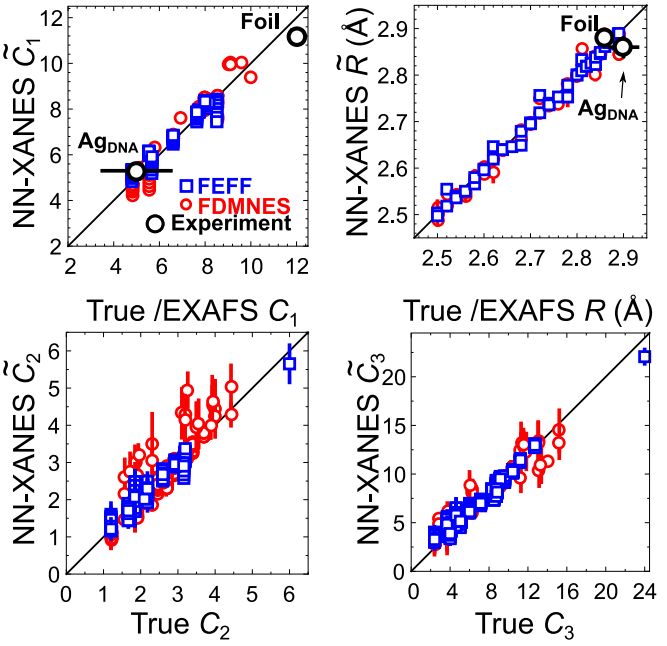

Fig. 2. Validation of NN accuracy with simulated particle-averaged XANES for particles of different sizes and shapes and with experimental data for reference samples. For simulated spectra the obtained results are compared with the known true values of corresponding structure parameters. For experimental spectra NN-XANES results are compared with those from EXAFS fitting (Roese et al., 2018).

C_1, C_2, C_3, R values for these models and NN yielded values $\tilde{C}_1$, $\tilde{C}_2$, $\tilde{C}_3$ and $\tilde{R}$ (Fig. 2) gives us confidence that the information about these structure parameters indeed is present in XANES data and can be extracted by NN method.

3. Experimental data

Ag clusters with sizes 2.0 ± 0.6 nm were produced in a supersonic expansion process (Hövel et al., 1993) and deposited into ionic liquid (Roese et al., 2018; Engemann et al., 2016). Temperature-controlled aggregation of the clusters was monitored using UV/vis spectroscopy (Roese et al., 2018). To investigate the changes in cluster local structure and morphology, in-situ XAS measurements were performed.

XAS data (Fig. 3) were collected at beamline P64 at DESY facility. The sample with ≈ 1 ppm Ag clusters in RTIL was filled into a liquid sample holder with Kapton windows, and its temperature was controlled using a circulation thermostat. XAS data for separated clusters were collected at 250 K. For this temperature cluster aggregation is not observed on a timescale of one day (according to UV/vis data) (Roese et al., 2018). Afterwards the sample was warmed up to room temperature, and UV/vis data were collected for 2.5 h in total during the aggregation process. In addition to XAS data for the sample at the end of this aggregation process, we also collected XAS for an "intermediate state" after 80 min at room temperature. Each time the sample was cooled again to 250 K to avoid aggregation during the XAS measurement. More details on sample preparation and characterization are given in Roese et al. (2018).

In addition, we analyze also XANES data for two reference samples: Ag foil and sub-nanometer Ag cluster sample (Ag_{DNA}), prepared by DNA assisted synthesis (Gwinn et al., 2008; O'Neill et al., 2009). XAS data for the latter sample were collected at X18A beamline at NSLS facility. According to the indirect fluorescence measurements, Ag_{DNA} sample contains Ag clusters with 11–13 atoms.

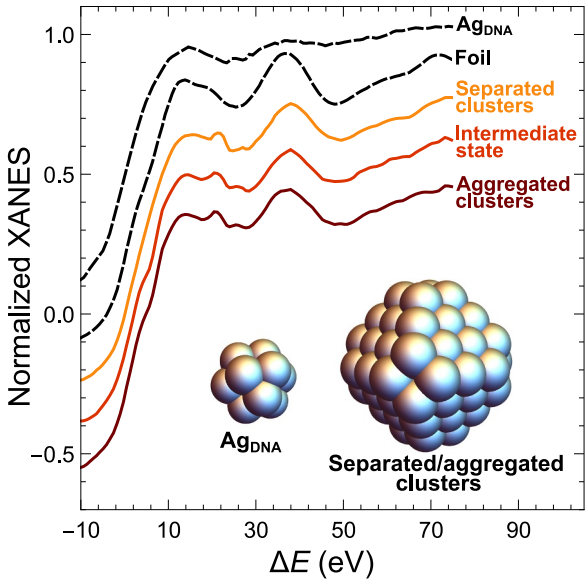

Fig. 3. Experimental in situ XANES data for Ag clusters (separated, partially aggregated, aggregated). Experimental data for Ag foil and for Ag_{DNA} sample are shown as references. Spectra are shifted vertically for clarity. In the insets - possible structure models for Ag NPs, constructed using CNs from NN-XANES analysis.

4. Results and discussion

To demonstrate the accuracy of NN-XANES method, we first apply it to reference spectra for Ag foil and Ag_{DNA} sample. The obtained structure parameters yielded by NN are shown in Table 1. CNs and interatomic distances for bulk Ag are known from X-ray diffraction (Goon et al., 1957) and are also shown in Table 1. They agree well with the NN results. For Ag_{DNA} sample, in turn, in addition to XANES data, also EXAFS data were collected that allowed us to obtain independently CN and interatomic distance for the first coordination shell (Roese et al., 2018). As shown in Fig. 2, EXAFS and NN-XANES results are in a good agreement. Slightly smaller R value for Ag_{DNA} sample than for foil may be attributed to the shortening of interatomic distances with NPs size (Montano et al., 1984). CNs for the 2nd and 3rd coordination shells, yielded by NN for Ag_{DNA} sample, are significantly smaller than those for bulk Ag, in agreement with the expected small NPs size. To check if $\tilde{C}_1$, $\tilde{C}_2$ and $\tilde{C}_3$ values yielded by NN are realistic, we compare them with the CNs for a large set of NPs models that were used for NN training, and look for a model, for which $\sum_{i=1}^{3}(C_i - \tilde{C}_i)^2/\varepsilon_i^2$ is minimal (here ε is the statistical uncertainty of NN result). For Ag_{DNA} sample, the best agreement was obtained for cuboctahedral model with 13 atoms (Fig. 3). Corresponding CNs for this model are reported in Table 1, and for all coordination shells are indeed in a good agreement with NN result. The obtained model also agrees with the expected small size of Ag_{DNA} NPs, as confirmed by fluorescence measurements. Consistency of the results observed for sub-nanometer NPs as well as for bulk Ag gives us confidence in the accuracy of our approach in a broad range of NPs sizes.

Table 1
Structure parameters obtained by NN from experimental XANES for reference samples (Ag foil and Ag_{DNA}) and from in-situ XANES data for separated and aggregated Ag clusters in RTIL. Uncertainty of the last digit is given in parentheses. CNs corresponding to possible particle 3D models (Fig. 3) are also given for comparison.

Sample	$\tilde{C}_1$	$\tilde{C}_2$	$\tilde{C}_3$	$\tilde{R}$ (Å)
Foil	11.24(6)	5.7(4)	22.1(7)	2.883(7)
Ideal FCC	12	6	24	2.889 Goon et al. (1957)
Ag_{DNA}	5.3(2)	1.4(7)	8(2)	2.86(2)
Best model for Ag_{DNA}	5.5	1.8	3.7	
Separated clusters	8.3(3)	2.8(7)	14(1)	2.89(2)
Intermediate state	8.3(3)	1.4(7)	15(2)	2.91(1)
Aggregated clusters	8.6(2)	1.5(7)	14(1)	2.90(2)
Best model for separated/ aggregated clusters	8.5(4)	3.2(3)	11.5	

Finally, we discuss the results obtained from the in-situ XANES for separated and aggregated Ag clusters in RTIL. As shown in Fig. 3, these spectra are more similar to Ag foil spectrum, suggesting significantly larger NPs sizes in these samples than in Ag_{DNA} sample. Signal-to-noise ratio is poor in these spectra, which prohibits advanced EXAFS-based analysis. CNs obtained by NN-XANES method and reported in Table 1, in turn, are reasonable. As expected, all CNs values are in-between those for Ag foil and Ag_{DNA} samples. The obtained nearest-neighbor distance $\tilde{R}$ agrees with that for bulk Ag. The results, obtained for separated clusters, partially aggregated and completely aggregated NPs are very similar. Only a small increase in $\tilde{C}_1$ value can be observed. $\tilde{C}_2$ and $\tilde{C}_3$ (which are more sensitive to NPs size and shape Frenkel et al., 2011; Jentys, 1999) agree within error bars for all three cases. This is an indication that the NPs aggregation takes place without coalescence, and their local structure and shape are preserved during this process.

To identify a possible shape for Ag clusters in these samples, we perform similar analysis as was done above for Ag_{DNA} sample. One possible shape for a "representative" NP model that has the same CNs as those yielded by the NN analysis (Table 1) is the truncated octahedral particle with 79 atoms (Fig. 3). The obtained NPs size (ca. 1.2 nm) is also close to the expected size for separated clusters (2.0 ± 0.6 nm) (Roese et al., 2018). One should emphasize here, however, that the experimental spectra are averaged over contributions of many NPs with, likely, quite different sizes and shapes. The shape analysis based on CNs extracted from XANES (or EXAFS) data thus can yield only an effective NP shape, and can be misleading, if the distribution of NPs sizes and shapes is broad (Frenkel et al., 2011).

5. Conclusions

We employed NN-XANES method for the analysis of NPs shape from in-situ XANES data, collected during NPs aggregation. Our results suggest that NPs aggregation takes place without coalescence and that the local structure and shape of these particles is preserved. This study shows that even when EXAFS data are not available due to experimental challenges, quantitative information on materials structure can be, nevertheless, extracted from XANES data, and can be used for advanced analysis, such as determination of NPs shape. We envision that our approach will be necessary in many cases, where the detailed knowledge of NPs structure and morphology is important, such as studies of heterogenous catalysts and plasmonic materials.

Acknowledgements

A. I. F. acknowledges support by the U.S. Department of Energy, Office of Basic Energy Sciences under Grant No. DE-FG02-03ER15476. A. I. F. acknowledges support by the Laboratory Directed Research and Development Program through LDRD 18-047 of Brookhaven National Laboratory under U.S. Department of Energy Contract No. DE-SC0012704 for initiating his research in machine learning methods. Parts of this research were carried out at P64 at DESY, a member of the Helmholtz Association (HGF). We thank V. Murzin, L. A. Martín-Montoya, and W. Caliebe for assistance in using beamline P64. Precharacterization of the samples by XANES measurements was performed at the Ag L_3-edge at BL8, DELTA, Technische Universität Dortmund, Germany, The authors thank Dr. D. Nykypanchuk from the Center for Functional Nanomaterials at Brookhaven National Laboratory for providing the Ag sample prepared by DNA templated synthesis. This research used resources of the Center for Functional

Nanomaterials, which is a U.S. DOE Office of Science Facility, and beamline X18A of the National Synchrotron Light Source at Brookhaven National Laboratory under Contract DE-SC0012704.

References

Behafarid, F., Ono, L., Mostafa, S., Croy, J., Shafai, G., Hong, S., Rahman, T., Bare, S.R., Roldan Cuenya, B., 2012. Electronic properties and charge transfer phenomena in pt nanoparticles on γ-Al_2O_3: size, shape, support, and adsorbate effects. Phys. Chem. Chem. Phys. 14, 11766–11779.

Bunău, O., Joly, Y., 2009. Self-consistent aspects of x-ray absorption calculations. J. Phys. Condens. Mat. 21, 345501.

Roldan Cuenya, B., Frenkel, A., Mostafa, S., Behafarid, F., Croy, J., Ono, L., Wang, Q., 2010. Anomalous lattice dynamics and thermal properties of supported size-and shape-selected Pt nanoparticles. Phys. Rev. B 82, 155450.

Roldan Cuenya, B., Ortigoza, M.A., Ono, L., Behafarid, F., Mostafa, S., Croy, J., Paredis, K., Shafai, G., Rahman, T., Li, L., et al., 2011. Thermodynamic properties of Pt nanoparticles: size, shape, support, and adsorbate effects. Phys. Rev. B 84, 245438.

Roldan Cuenya, B., 2012. Metal nanoparticle catalysts beginning to shape-up, Accounts Chem. Res 46, 1682–1691.

Engemann, D.C., Roese, S., Hövel, H., 2016. Preformed 2 nm Ag clusters deposited into ionic liquids: stabilization by cation-cluster interaction. J. Phys. Chem. C. 120, 6239–6245.

Frenkel, A.I., Hills, C.W., Nuzzo, R.G., 2001. A view from the inside: complexity in the atomic scale ordering of supported metal nanoparticles. J. Phys. Chem. B 105, 12689–12703.

Frenkel, A.I., Yevick, A., Cooper, C., Vasic, R., 2011. Modeling the structure and composition of nanoparticles by extended x-ray absorption fine-structure spectroscopy. Annu. Rev. Anal. Chem. 4, 23–39.

Frenkel, A.I., 1999. Solving the structure of nanoparticles by multiple-scattering EXAFS analysis. J. Synchrotron Radiat. 6, 293–295.

Glasner, D., Frenkel, A.I., 2007. Geometrical characteristics of regular polyhedra: application to EXAFS studies of nanoclusters. AIP Conf. Proc. 882, 746–748.

Goon, E.J., Mason, J.T., Gibb Jr, T.R., 1957. X-ray powder diffraction assembly for studies at elevated temperatures and high gas pressures. Rev. Sci. Instrum. 28, 342–344.

Grunwaldt, J.-D., Molenbroek, A., Topsœ, N.-Y., Topsœ, H., Clausen, B., 2000. In situ investigations of structural changes in Cu/ZnO catalysts. J. Catal. 194, 452–460.

Gwinn, E.G., O'Neill, P., Guerrero, A.J., Bouwmeester, D., Fygenson, D.K., 2008. Sequence-dependent fluorescence of DNA-hosted silver nanoclusters. Adv. Mater. 20, 279–283.

Hövel, H., Fritz, S., Hilger, A., Kreibig, U., Vollmer, M., 1993. Width of cluster plasmon resonances: bulk dielectric functions and chemical interface damping. Phys. Rev. B 48, 18178.

Hansen, P.L., Wagner, J.B., Helveg, S., Rostrup-Nielsen, J.R., Clausen, B.S., Topsœ, H., 2002. Atom-resolved imaging of dynamic shape changes in supported copper nanocrystals. Science 295, 2053–2055.

Jentys, A., 1999. Estimation of mean size and shape of small metal particles by EXAFS. Phys. Chem. Chem. Phys. 1, 4059–4063.

Kelly, K.L., Coronado, E., Zhao, L.L., Schatz, G.C., 2003. The optical properties of metal nanoparticles: the influence of size, shape, and dielectric environment. J. Phys. Chem. B 107, 668–677.

LeCun, Y., Bengio, Y., Hinton, G., 2015. Deep learning. Nature 521, 436.

Montano, P., Schulze, W., Tesche, B., Shenoy, G., Morrison, T., 1984. Extended x-ray-absorption fine-structure study of Ag particles isolated in solid argon. Phys. Rev. B 30, 672.

Mostafa, S., Behafarid, F., Croy, J.R., Ono, L.K., Li, L., Yang, J.C., Frenkel, A.I., Roldan Cuenya, B., 2010. Shape-dependent catalytic properties of Pt nanoparticles. J. Am. Chem. Soc. 132, 15714–15719.

Narayanan, R., El-Sayed, M.A., 2004. Shape-dependent catalytic activity of platinum nanoparticles in colloidal solution. Nano Lett. 4, 1343–1348.

Newton, M.A., Belver-Coldeira, C., Martínez-Arias, A., Fernández-García, M., 2007. Dynamic in situ observation of rapid size and shape change of supported Pd nanoparticles during CO/NO cycling. Nat. Mater. 6, 528.

O'Neill, P.R., Velazquez, L.R., Dunn, D.G., Gwinn, E.G., Fygenson, D.K., 2009. Hairpins with poly-C loops stabilize four types of fluorescent Ag_n:DNA. J. Phys. Chem. C 113, 4229–4233.

Porsgaard, S., Merte, L.R., Ono, L.K., Behafarid, F., Matos, J., Helveg, S., Salmeron, M., Roldan Cuenya, B., Besenbacher, F., 2012. Stability of platinum nanoparticles supported on SiO_2/Si (111): a high-pressure x-ray photoelectron spectroscopy study. ACS Nano 6, 10743–10749.

Rehr, J.J., Kas, J.J., Vila, F.D., Prange, M.P., Jorissen, K., 2010. Parameter-free calculations of x-ray spectra with FEFF9. Phys. Chem. Chem. Phys. 12, 5503–5513.

Roese, S., Kononov, A., Timoshenko, J., Frenkel, A.I., Hövel, H., 2018. Cluster assemblies produced by aggregation of preformed Ag clusters in ionic liquids. Langmuir 34, 4811–4819.

Roldan Cuenya, B., Croy, J.R., Mostafa, S., Behafarid, F., Li, L., Zhang, Z., Yang, J.C., Wang, Q., Frenkel, A.I., 2010. Solving the structure of size-selected Pt nanocatalysts synthesized by inverse micelle encapsulation. J. Am. Chem. Soc. 132, 8747–8756.

Tao, A.R., Habas, S., Yang, P., 2008. Shape control of colloidal metal nanocrystals. Small 4, 310–325.

Timoshenko, J., Lu, D., Lin, Y., Frenkel, A.I., 2017. Supervised machine-learning-based determination of three-dimensional structure of metallic nanoparticles. J. Phys. Chem. Lett. 8, 5091–5098.

Timoshenko, J., Halder, A., Yang, B., Seifer, S., Frenkel, A.I., 2018. Subnanometer substructures in nanoassemblies formed from clusters under reactive atmosphere revealed using machine learning. J. Phys. Chem. C 122, 21686–21693.

Van Bokhoven, J.A., Lamberti, C., 2016. X-ray absorption and X-ray emission spectroscopy: theory and applications 1 John Wiley & Sons.